2

Quantum Measurement and Sub-Band Tunneling in Double Quantum Dots

Héctor Cruz
Universidad de La Laguna
Spain

1. Introduction

Quantum dots have attracted significant interest in recent years. Quantum dots attractive candidates as the building blocks for a quantum computer due to their potential to readily scale. The number of electrons can be reduced down to one in a gate-defined quantum dot.

High frequency operations on quantum dot systems have been used to observe new phenomena such as coherent charge oscillations and elastic tunneling behavior. Observation of these phenomena is made possible by (*in situ*) control of the rate of tunneling Γ between the quantum dots.

Measurements with a noninvasive detector in a double quantum dot system (qubit) has been extensively realized (Astley et al., 2007). A group of electrons is placed in a double quantum dot, whereas the detector (a quantum point contact) is localized near one of the dots. The quantum point contact acts as a measuring device.

One remaining key question is the theoretical study of the tunneling dynamics after the observation in a double quantum dot system (Cruz, 2002). Electrons can be projected onto a well define quantum dot after the observation takes place, if we consider the two quantum dots highly isolated (Ferreira et al., 2010).

In addition, we know that if two electron subbands are occupied, the electrical properties can be strongly modified due to the carrier-carrier interaction between subbands (Shabami et al., 2010). In this work we shall extend the Coulomb effect analysis when two subbands are occupied in the quantum dots. Then, the tunneling process could be modified due to the using of two different wave functions for two electron groups that interact between each other.

2. Model

It has been found that there are two distinct energy bands within semiconductors. From experiments, it is found that the lower band is almost full of electrons and the conduct by the movement of the empty states. In a semiconductor, the upper band is almost devoid of electrons. It represents excited electron states promoted from localized covalent bonds into extended states. Such electrons contribute to the current flow. The energy difference between the two bands is known as the band gap. Effective masses of around $0.067m_0$ for an electron in the conduction bands and $0.6m_0$ for a hole in the valence band can be taken in GaAs.

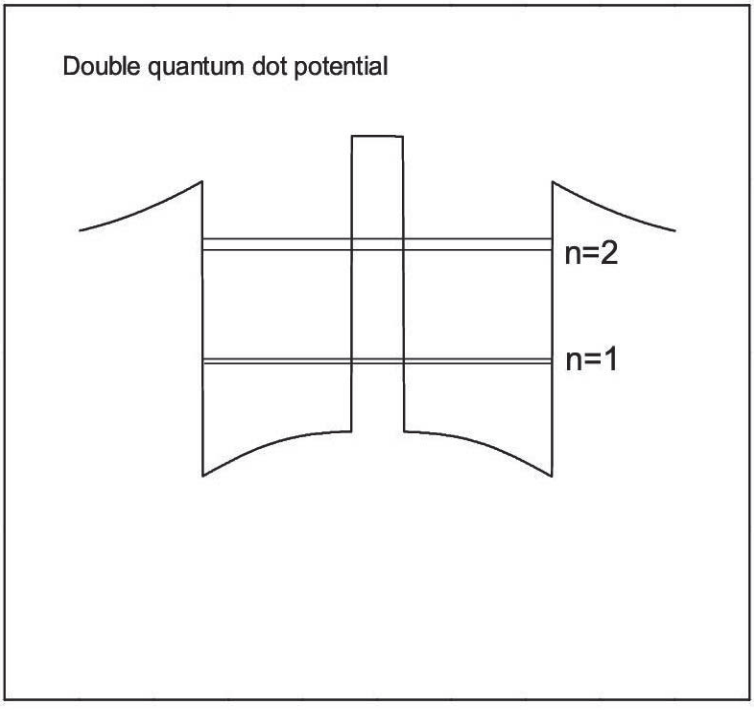

Fig. 1. A schematic illustration of the proposed experiment in the semiconductor quantum dot system. Double quantum dot system in absence of external bias.

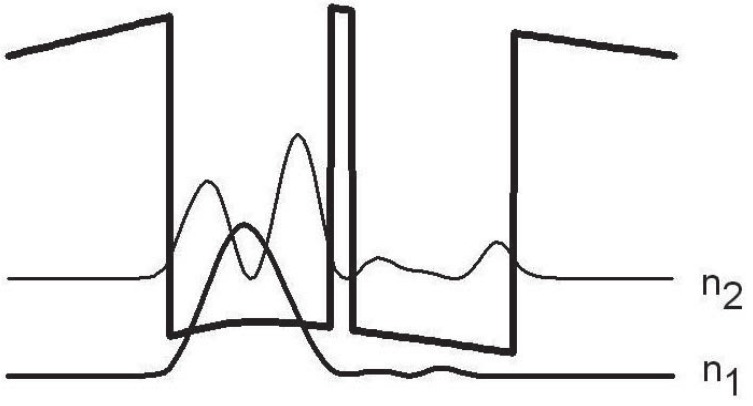

Fig. 2. Conduction band potential and carrier wave functions at $t = 0.1$ ps. We have taken an initial carrier density equal to $n_1 = 3.0 \times 10^{11}\text{cm}^{-2}$ and $n_2 = 0.0 \times 10^{11}\text{cm}^{-2}$.

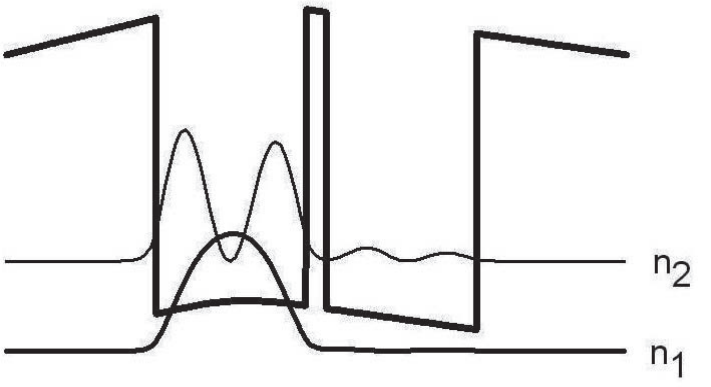

Fig. 3. Conduction band potential and carrier wave functions at $t = 0.2$ ps. We have taken an initial carrier density equal to $n_1 = 3.0 \times 10^{11}\text{cm}^{-2}$ and $n_2 = 0.0 \times 10^{11}\text{cm}^{-2}$.

The effective mass approximation is for a bulk crystal. The crystal is so large with respect to the scale of an electron wave function that is efectively infinite. In such a case, The Schrödinger equation has been found to be as follows:

$$-\frac{\hbar^2}{2m^*}\frac{\partial^2}{\partial z^2}\psi(z) = E\psi(z) \tag{1}$$

This equation is valid when two materials are placed adjacent to each other to form a heterojunction. The effective mass could be a function of the position and the band gaps of the materials can also be different. The discontinuity can be represented by a constant potential term. Thus the Schrödinger equation would be generalized to

$$-\frac{\hbar^2}{2m^*}\frac{\partial^2}{\partial z^2}\psi(z) + V(z)\psi(z) = E\psi(z) \tag{2}$$

The one dimensional potential $V(z)$ represents the band discontinuities at the heterojunction. The one dimensional potential is constructed from alternanting layers of dissimilar semiconductors, then the eletron or hole can move in the plane of the layers.

In this case, all the terms of the kinetic operator are required, and the Schrödinger equation would be as follows:

$$-\frac{\hbar^2}{2m^*}\left(\frac{\partial^2}{\partial x^2}\psi + \frac{\partial^2}{\partial y^2}\psi + \frac{\partial^2}{\partial z^2}\psi\right) + V(z)\psi = E\psi \tag{3}$$

As the potential can be written as a sum of independent functions, i.e.

$$V = V(x) + V(y) + V(z) \tag{4}$$

the eigenfunction of the system can be written as:

$$\psi(x, y, z) = \psi_x(x)\psi_y(y)\psi_z(z) \tag{5}$$

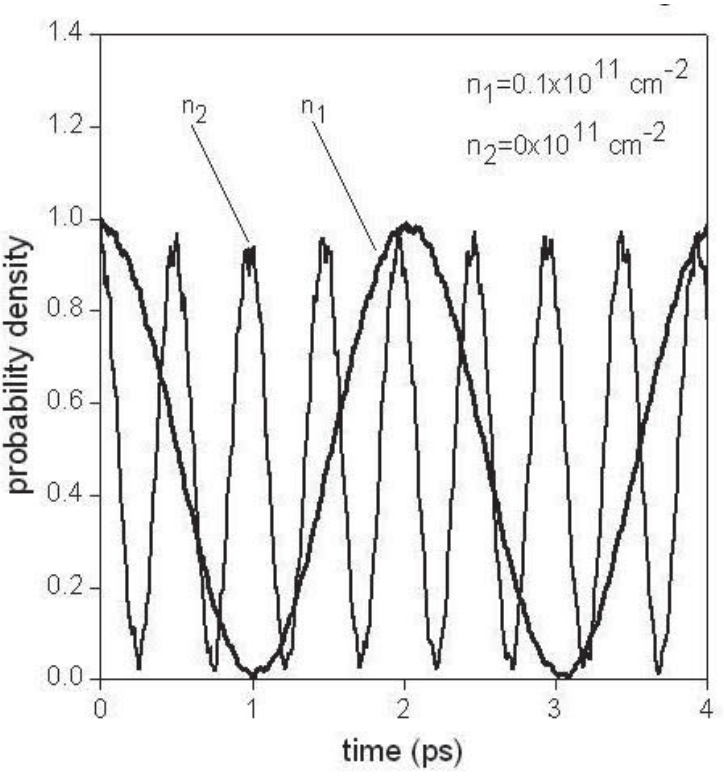

Fig. 4. Probability density in the left quantum well versus time at different carrier densities. $n_1 = 0.1 \times 10^{11}$ cm^{-2} and $n_2 = 0 \times 10^{11}$ cm^{-2}.

and using this in the above Schrödinger equation, then:

$$-\frac{\hbar^2}{2m^*}\left(\frac{\partial^2\psi_x}{\partial x^2}\psi_y\psi_z + \frac{\partial^2\psi_y}{\partial y^2}\psi_x\psi_z + \frac{\partial^2\psi_z}{\partial z^2}\psi_x\psi_y\right) + V(z)\psi_x\psi_y\psi_z = E\psi_x\psi_y\psi_z \tag{6}$$

The last component is identical to a one-dimensional equation for a confining potential $V(z)$. The x and y components represent a moving particle and the wave function must reflect a current flow and have complex components. Then,

$$-\frac{\hbar^2}{2m^*}\frac{\partial^2}{\partial x^2}e^{ik_x x} = E_x e^{ik_x x} \tag{7}$$

and thus,

$$-\frac{\hbar^2}{2m^*}\frac{\partial^2}{\partial y^2}e^{ik_y y} = E_y e^{ik_y y} \tag{8}$$

where

$$\frac{\hbar^2}{2m^*}{k_x}^2 = E_x \tag{9}$$

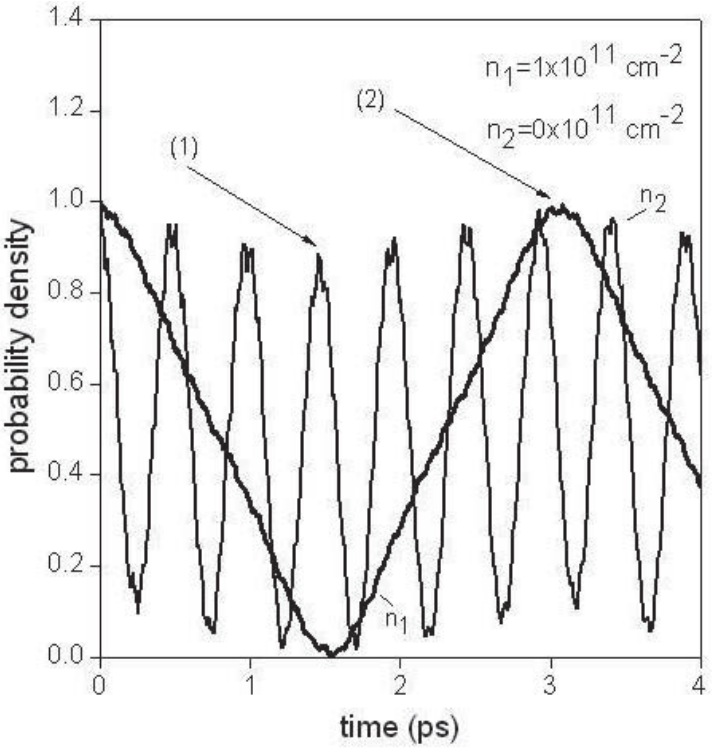

Fig. 5. Probability density in the left quantum well versus time at different carrier densities. $n_1 = 1 \times 10^{11}$ cm^{-2} and $n_2 = 0 \times 10^{11}$ cm^{-2}.

and

$$\frac{\hbar^2}{2m^*} k_y{}^2 = E_y \tag{10}$$

An infinity extent in the $x - y$ plane can be summarized as:

$$\psi_{x,y}(x,y) = \frac{1}{A} e^{i(k_x x + k_y y)} \tag{11}$$

and

$$E_{x,y} = \frac{\hbar^2 k_{x,y}^2}{2m^*} \tag{12}$$

Therefore, while solutions of the Schrödinger equation along the axis of the one-dimensional produce discrete states of energy E_z in the plane of a semiconductor quantum well, there is a continuous range of allowed energies.

In order to study the dynamics in the quantum well direction, we need to solve the time-dependent Schrödinger equation associated with an electron in a well potential for each

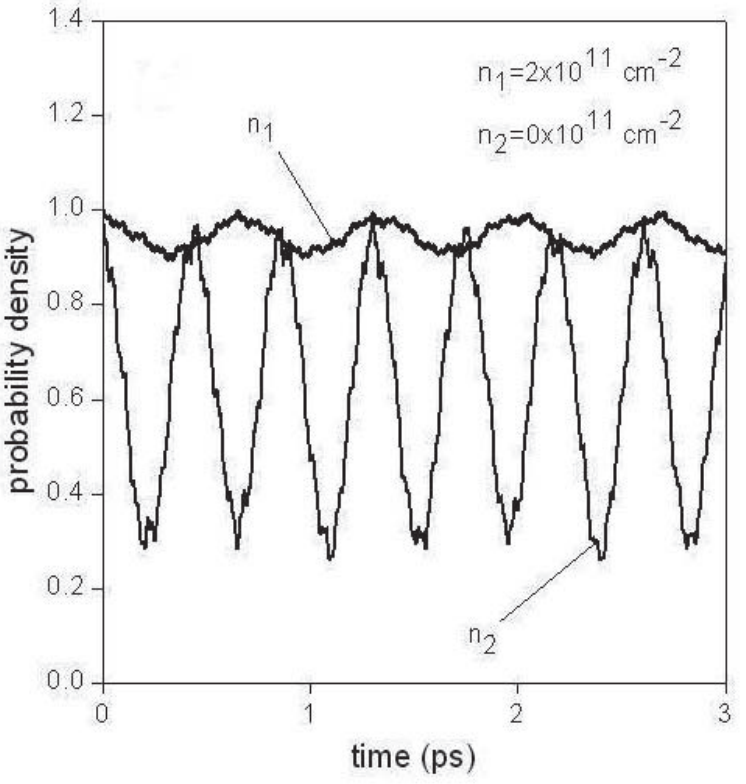

Fig. 6. Probability density in the left quantum well versus time at different carrier densities. $n_1 = 2 \times 10^{11}$ cm^{-2} and $n_2 = 0 \times 10^{11}$ cm^{-2}.

subband. The ψ_{n_1} and ψ_{n_2} wave functions for each conduction subband in the z axis will be given by the nonlinear Schrödinger equations Cruz (2011)

$$i\hbar \frac{\partial}{\partial t}\psi_{n_1}(z,t) = \left[-\frac{\hbar^2}{2m^*}\frac{\partial^2}{\partial z^2} + V(z) + V_H\left(\mid \psi_{n_1} \mid^2, \mid \psi_{n_2} \mid^2 \right) \right] \psi_{n_1}(z,t), \tag{13}$$

$$i\hbar \frac{\partial}{\partial t}\psi_{n_2}(z,t) = \left[-\frac{\hbar^2}{2m^*}\frac{\partial^2}{\partial z^2} + V(z) + V_H\left(\mid \psi_{n_1} \mid^2, \mid \psi_{n_2} \mid^2 \right) \right] \psi_{n_2}(z,t), \tag{14}$$

where the subscripts n_1 and n_2 refer to the subband number, respectively, and $V(z)$ is the potential due to the quantum wells. The m^* is the electron effective mass. V_H is the Hartree potential given by the electron-electron interaction in the heterostructure region. Such a many-body potential is given by Poisson's equation Cruz (2002)

$$\frac{\partial^2}{\partial z^2} V_H(z,t) = -\frac{e^2}{\varepsilon}\left[n_1 \mid \psi_{n_1}(z,t) \mid^2 + n_2 \mid \psi_{n_2}(z,t) \mid^2 \right], \tag{15}$$

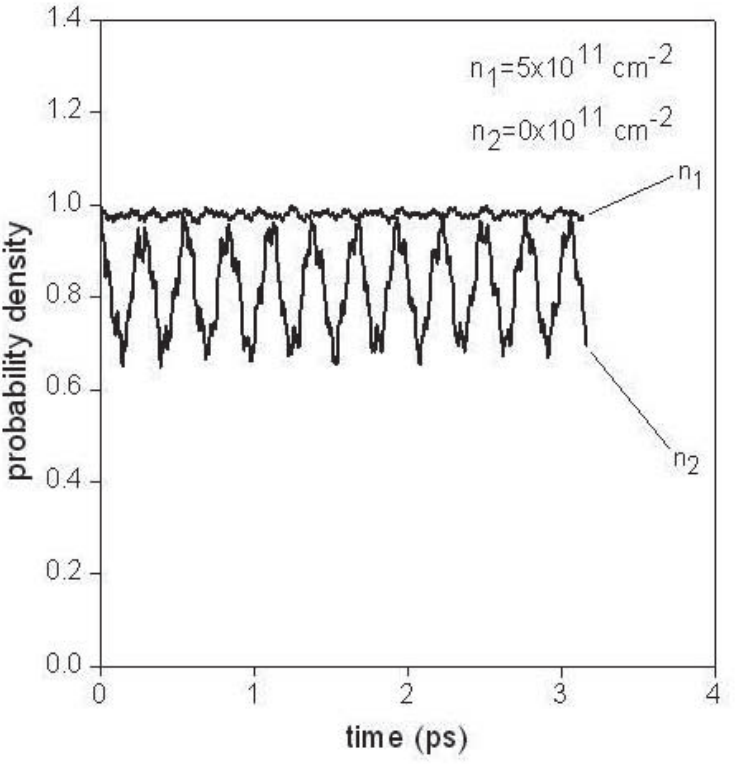

Fig. 7. Probability density in the left quantum well versus time at different carrier densities. $n_1 = 5 \times 10^{11}$ cm^{-2} and $n_2 = 0 \times 10^{11}$ cm^{-2}.

where ε is the GaAs dielectric constant and n_1 and n_2 are the carrier sheet densities in each subband. Considering the Fermi energy ε_F, the carrier densities can be easily calculated. If $\varepsilon_F < \varepsilon_2$, we have

$$n_1 = (\varepsilon_F - \varepsilon_1)\rho_0 \tag{16}$$

and $n_2 = 0$ and if $\varepsilon_F > \varepsilon_2$, we have

$$n_1 = (\varepsilon_F - \varepsilon_1)\rho_0 \tag{17}$$

and

$$n_2 = (\varepsilon_F - \varepsilon_2)\rho_0. \tag{18}$$

In such a case, L is the quantum well width,

$$\varepsilon_n = \hbar^2 n^2 \pi^2 / 2m^* L^2 \tag{19}$$

approaches the quantum well energy levels and

$$\rho_0 = m^* / \pi\hbar^2 \tag{20}$$

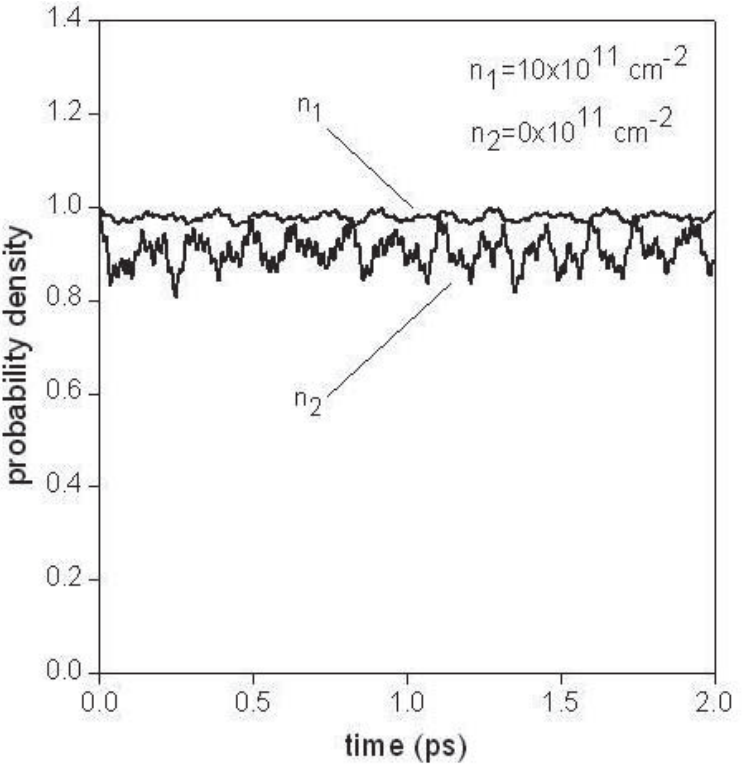

Fig. 8. Probability density in the left quantum well versus time at different carrier densities. $n_1 = 10 \times 10^{11}$ cm^{-2} and $n_2 = 0 \times 10^{11}$ cm^{-2}.

is the two dimensional density of states at zero temperature.

Now we discretize time by a superscript ϑ and spatial position in the subbands by a subscript ξ and φ, respectively. Thus,

$$\psi_{n_1} \rightarrow \psi_{\xi}^{\vartheta} \tag{21}$$

and

$$\psi_{n_2} \rightarrow \psi_{\varphi}^{\vartheta}. \tag{22}$$

The various z values become $\xi\delta z$ in the conduction band and $\varphi\delta z$, where δz is the mesh width.

Similarly, the time variable takes the values $\vartheta\delta t$, where δt is the time step. We have used a unitary propagation scheme for the evolution operator obtaining a tridiagonal linear system that can be solved by using the split-step method Cruz (2002).

In the split-step approach, both wave packets are advanced in time steps δt short enough that the algorithm

$$e^{-i\delta t T_H/2} e^{-i\delta t U} e^{-i\delta t T_H/2} \tag{23}$$

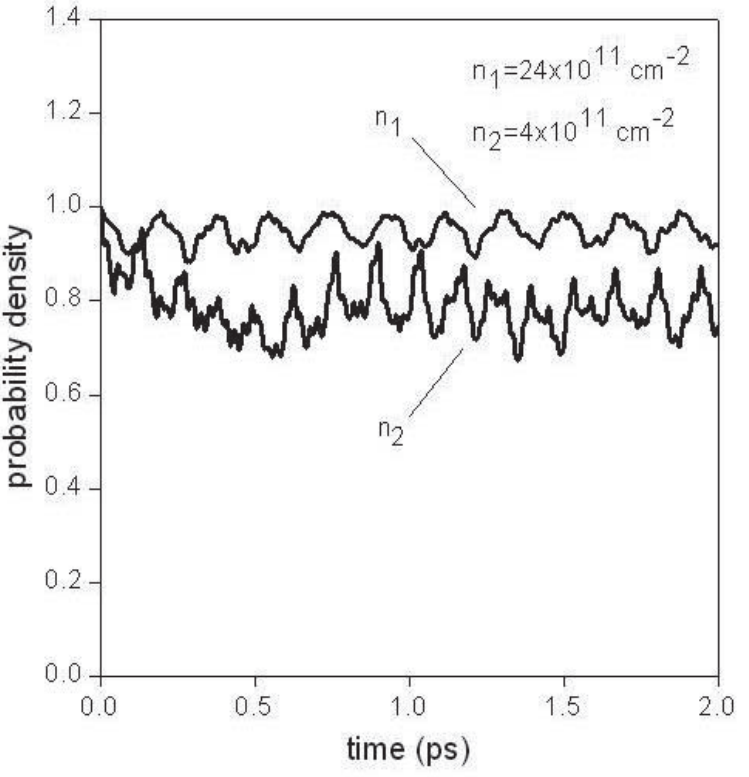

Fig. 9. Probability density in the left quantum well versus time at different carrier densities. $n_1 = 24 \times 10^{11}$ cm^{-2} and $n_2 = 4 \times 10^{11}$ cm^{-2}.

can be applied to the generator. T_H and U are the Hamiltonian kinetic and potential terms.

Then, Poisson's equation associated with V_H is solved using another tridiagonal numerical method for each δt value. In each time step δt, the algorithm propagates the wave packets freely for $\delta t/2$, applies the full potential interaction, then propagates freely for the remaining $\delta t/2$. The split-step algorithm is stable and norm preserving and it is well suited to time-dependent Hamiltonian problems.

We have numerically integrated Eqs. (13), (14) and (15) using $n_1 = 3.0 \times 10^{11}$ cm^{-2} and $n_2 = 0.0 \times 10^{11}$ cm^{-2} carrier densities. In our calculations, we shall consider a GaAs double quantum dot system. We have assumed that both ψ_{n_1} and ψ_{n_2} wave functions are initially created in the center of the left quantum well at $t = 0$ in our model (Fig. 1).

Then, the equations are numerically solved using a spatial mesh size of 0.5Å, a time mesh size of 0.2 a.u and a finite box (5,000Å) large enough as to neglect border effects. The electron effective-mass is taken to be $0.067m_0$ and L=150 Å. The barrier thickness is 20 Å.

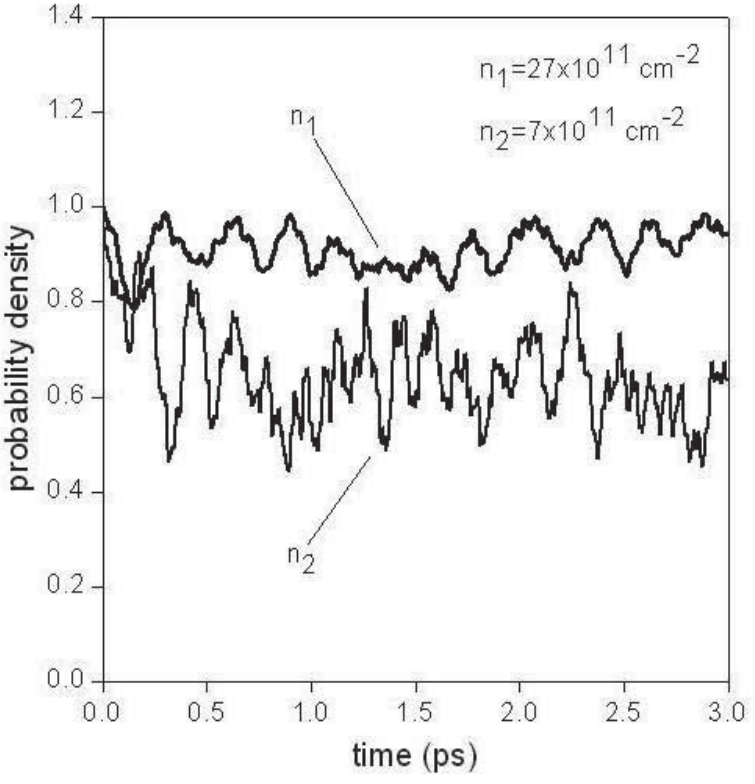

Fig. 10. Probability density in the left quantum well versus time at different carrier densities. $n_1 = 27 \times 10^{11}$ cm^{-2} and $n_2 = 7 \times 10^{11}$ cm^{-2}.

3. Results

The numerical integration in time allows us to obtain the carrier probability, P, in a defined semiconductor region $[a, b]$ and electron subband at any time t

$$P_{n_1,n_2}(t) = \int_a^b dz \, |\psi_{n_1,n_2}(z,t)|^2, \tag{24}$$

where $[a,b]$ are the quantum well limits. In Fig. 4-10 we have plotted the electron probability density in the left quantum well versus time at different electronic sheet densities.

The charge density values were obtained through Eq. (24). The existence of tunneling oscillations between both quantum wells at low densities is shown in Fig. 4. In Fig. 4 it is found that the amplitude of the oscillating charge density is approximately equal to 1 at resonant condition.

The electron energy levels of both wells are exactly aligned at $n_1 = 0.0 \times 10^{11}$cm^{-2} and $n_2 = 0.0 \times 10^{11}$cm^{-2} (Fig. 1) in the conduction band. In our case, the total charge density

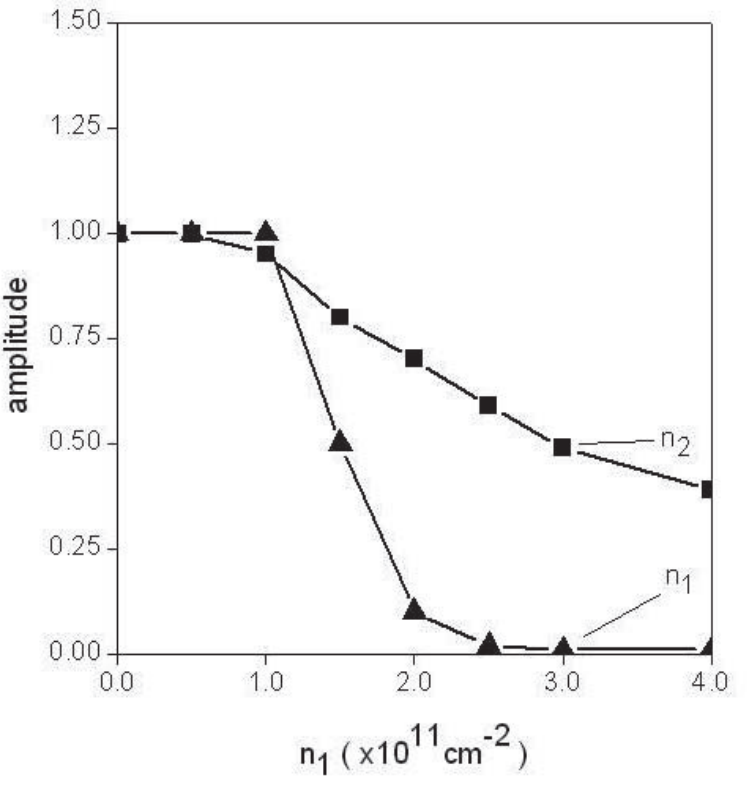

Fig. 11. Amplitude of the tunneling oscillations versus carrier sheet density. Triangles: first subband. Squares: second subband.

will oscillate between both wells with a certain tunneling period due to $n_1 \sim 0$ ($n_1 = 0.1 \times 10^{11}\text{cm}^{-2}$).

The level splitting between both quantum wells is proportional to the inverse of the tunneling period. The subsequent evolution of the wave function will basically depend on such a value of the level splitting. However, the quantum well eigenvalues are not aligned for a higher n_1 value, Fig. 5. Then, the amplitude of the oscillating charge is not always equal to 1.

When the n_1 wave function is in the right quantum well, P_{n_2} is never equal to 1, see the arrow (1) in Fig. 5. And when the n_1 wave function is in the left quantum well, P_{n_2} is never equal to 0, see the arrow (2) in Fig. 5.

In such a case, the charge dynamically trapped in the double-well system produces a reaction field which modifies the P_{n_2} value of the charge density oscillations for both wave packets. As a result, the averaged amplitude of the oscillating charge density is never equal to 1, Fig. 5.

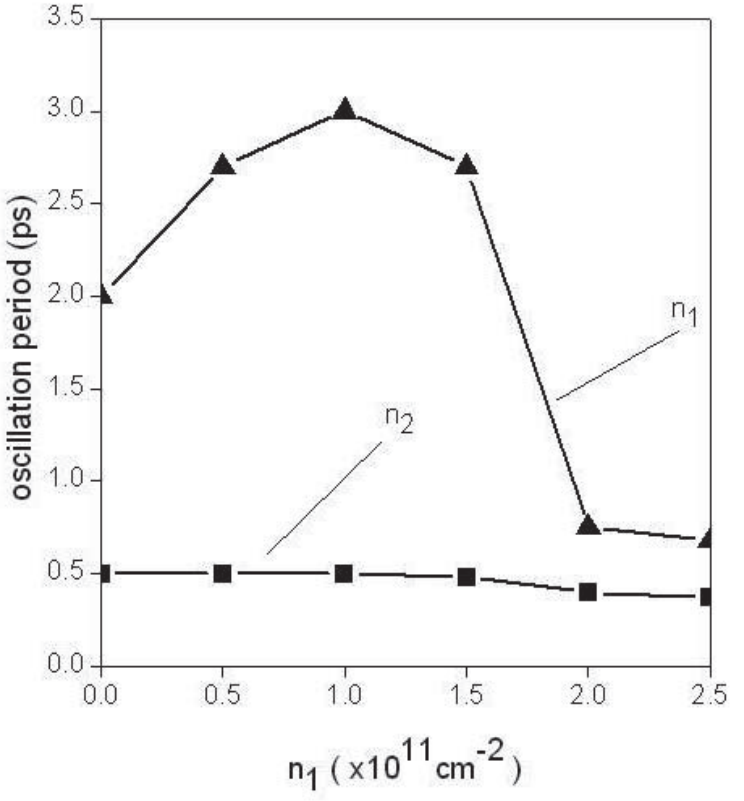

Fig. 12. Period of the tunneling oscillations versus carrier sheet density. Triangles: first subband. Squares: second subband.

Now we plot the averaged amplitude of the tunneling oscillations versus n_1 for low ε_F values, i.e., $\varepsilon_F < \varepsilon_2$ in Fig. 11. At $n_2 = 0.0 \times 10^{11}\text{cm}^{-2}$, it is found that the amplitude of the tunneling oscillations for both wave packets decreases as we increase n_1.

Such a new nonlinear effect is given by the n_1 charge density. The n_2 curve decrease is less than that obtained in the n_1 case in Fig. 11. Such a result can be easily explained as follows. If the potential difference between both wells is higher than the level splitting, the resonant condition is not obtained, and then the tunnelling process is not allowed.

The level splitting in the first subband is much smaller than in the second subband case due to the different barrier transparency, Fig. 1. We can notice that the barrier transparency increases as we increase the energy in a double quantum well. Then, the nonlinear effects are more important in the n_1 case.

We plot the period of the tunneling oscillations versus the n_1 carrier sheet density at $n_2 = 0.0 \times 10^{11}\text{cm}^{-2}$ in Fig. 12. It is found that the oscillation period of the first subband is always

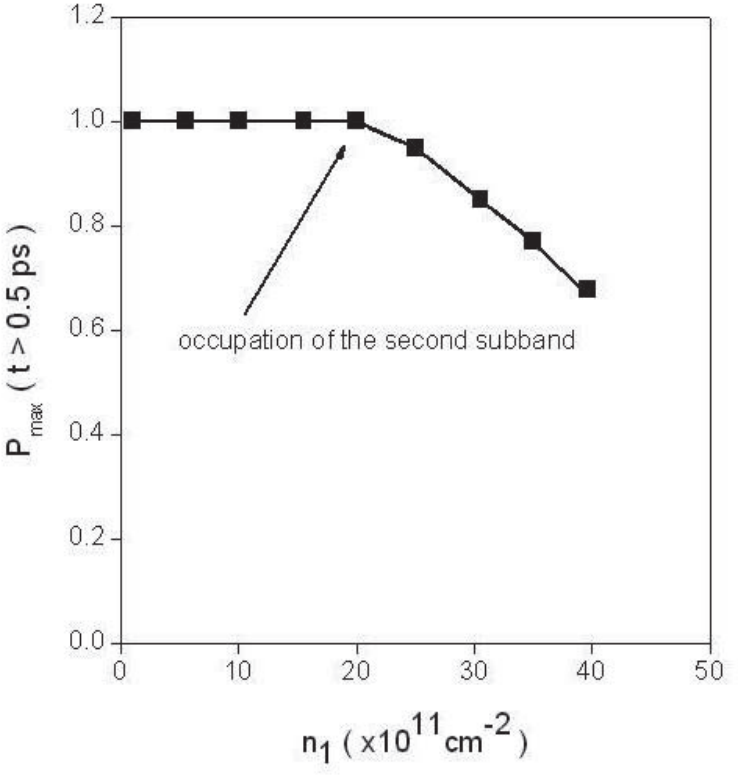

Fig. 13. The maximum probability density in the left quantum well for the second subband after a small initial period ($t > 0.5ps$)

higher than in the n_2 case. Such a result can be explained as follows. We know that the electron tunneling time between two quantum wells decreases as we increase energy.

The electrons in the second subband have higher energy, and an smaller oscillation period, than the n_1 electrons. The tunneling time in the first subband is strongly affected by the n_1 charge density. As a consequence, the nonlinear effects are more important in the n_1 case due to the level splitting in the first subband is much smaller.

In addition to this, and if the number of electrons is large enough, both electron subbands can be occupied. In such a case, we have intersubband interaction, i.e., $n_1 > 0$ and $n_2 > 0$ ($\varepsilon_F > \varepsilon_2$) in Fig. 9-10. Important nonlinear effect in the tunneling oscillations between both quantum wells, which modifies the dynamical evolution of the system, are shown.

The time-dependent evolution of the electron wave packets is strongly modified due to the repulsive intersubband interaction between both wave functions at $\varepsilon_F > \varepsilon_2$ values. We have two different wave functions for two electron groups that interact between each other.

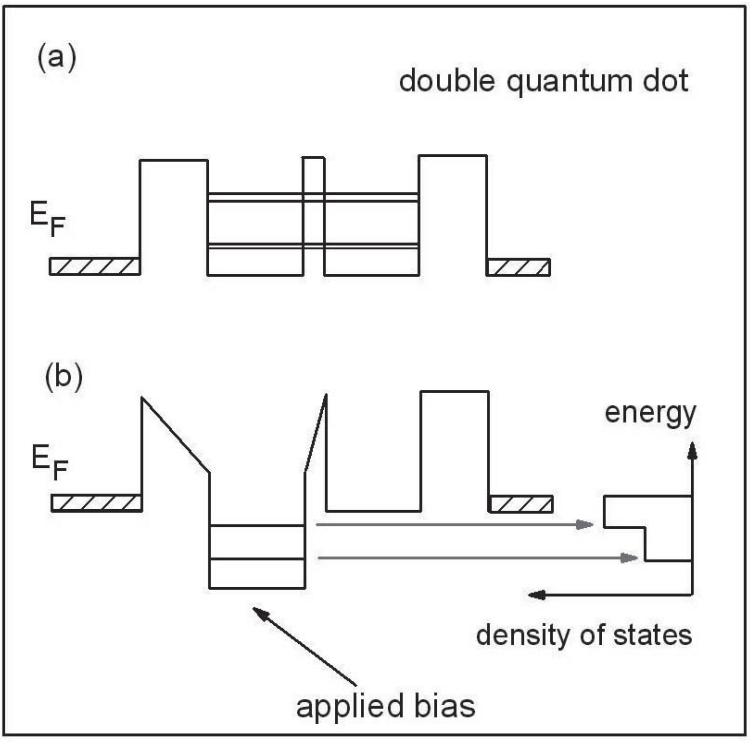

Fig. 14. A schematic illustration of the proposed experiment (a) Double quantum dot system in absence of external bias. (b) The electrons in the left reservoir can tunnel into the left dot when an external voltage is applied to the left quantum well. The density of states is filled up to the Fermi energy ε_F. As a consequence, electrons can be initially injected in the left quantum dot.

The charge dynamically trapped in the double-well system produces a reaction field which modifies the form of the probability curves for both ψ_{n_1} and ψ_{n_2}. As a result we have found important nonlinear effects in the tunneling dynamics for both subbands in Fig. 10.

The amplitude of the oscillating charge density is never equal to 1 in the second subband at high n_1 and n_2 values after a small initial period (t >0.5 ps). We plot P_{max} the maximum probability density in the left quantum well for the second subband after a small initial period ($t > 0.5$ ps) in Fig. 13. It is shown that the P_{max} value is decreased as we increase n_1.

As we increase both n_1 and n_2 values, the nonlinear effects due to the repulsive intersubband interaction are increased. At $\varepsilon_F > \varepsilon_2$ values, it is found that the symmetry of the oscillations is broken due to the nonlinear effects (Fig. 10).

As a result, it is shown the possibility of suppression of the tunneling oscillations in the double quantum well system in the $\varepsilon_F > \varepsilon_2$ regime ($n_1 > 20.0 \times 10^{11}$ cm^{-2}), Fig. 13. We explain this effect by considering our nonlinear effective-mass Schrödinger equations. In absence of

intersubband interaction, i.e., $n_1 > 0$ and $n_2 = 0$, we know that the maximum P value of the oscillating charge density is approximately equal to 1 at low n_1 values, Fig. 4.

In such a case, the nonlinear effects are generated by a single charge distribution. However, and at high n_1 and n_2 values, we have a reaction field generated by two charge distributions. If two subbands are occupied, important nonlinear effects in the carrier dynamics are obtained (Fig. 10).

As it is shown in Fig. 1, electrons can be initially distributed in both subbands. The electrons in the left reservoir can tunnel into the left dot, Fig. 14, when an external voltage is applied to the left quantum well. Then, the quantum states in the left quantum well are filled up to the Fermi energy. If we now switch off the applied voltage, Fig. 14, we obtain electrons distributed in both subbands that are localized in the left quantum well.

The initial wave functions $\psi_{n_1}(t = 0)$ and $\psi_{n_2}(t = 0)$ correspond to quantum well eigenstates in the left dot. In such experiment, the superposition of both symmetric and antisymmetric quantum-well eigenstates in the conduction band leads to coherent tunneling between both quantum wells. We have two different charge densities that oscillate with different tunneling periods.

4. Conclusion

In this work, we have studied the post-measurement dynamics in a double quantum dot system considering two subband wave packets. We have numerically integrated in space and time the effective-mass Schrödringer equation for two electron gases in a double quantum dot system.

We found two time-varying moments in the nanostructure with two different frequencies. In addition, it is found important nonlinear effects if two electron subbands are occupied. The symmetry of the tunneling oscillation can be broken due to nonlinear effects at high charge density values.

5. References

Astley, M. R.; Kataoka, M.; Ford, C. B. J.; Barnes, C. H. W., Anderson, D., Jones, G. A. C.; Farrer, I.; Ritchie, D. A. & Pepper, M. (2007). Energy-Dependent Tunneling from Few-Electron Dynamic Quantum Dots. *Physical Review Letters*. Vol. 99, 156802-156806, ISBN 0031-9007/07/99(15)/156802(4)

Cruz, H. (2002). Tunneling and time-dependent magnetic phase transitions in a bilayer electron system. *Physical Review B*, Vol. 65, 245313-245318, ISBN 0163-1829/2002/65(24)/245313(5)

Cruz, H. & Luis, D. (2011). Coulomb effects and sub-band tunneling in quantum wells. *Journal of Applied Physics*, Vol. 109, 073725-073729, ISBN 0021-8979/2011/109(7)/073725(5)

Ferreira, G. P.; Freire, H. J. P. & Egues, J. C. (2010). Many-Body Effects on the ρ_{xx} Ringlike Structures in Two-Subband Wells. *Physical Review Letters*. Vol. 104, 066803-066807, ISBN 0031-9007/10/104(6)/066803(4)

Shabami, J.; Lin, Y. & Shayegan, M. (2010). Quantum Coherence in a One-Electron Semiconductor Charge Qubit. *Physical Review Letters*, Vol. 105, 246804-246808, ISBN 0031-9007/10/105(24)/246804(4)

Van der Wiel, W. G.; De Franceschi, S.; Elzerman J. M.; Fujisawa, T.; Tarucha, S. & Konwenhoven, L. P. (2003). Electron transport through double quantum dots. *Review of Modern Physics*, Vol. 75, No. 1, 1-22, ISBN 0034-6861/2003/75(1)/1(22)